EMBO reports

scientific report

# ARE-mRNA degradation requires the 5′–3′ decay pathway

*Georg Stoecklin*[+], *Thomas Mayo & Paul Anderson*

Division of Rheumatology, Immunology & Allergy, Brigham & Women's Hospital, Harvard Medical School, Boston, Massachusetts, USA

**As an important mode of suppressing gene expression, messenger RNAs containing an AU-rich element (ARE) in the 3′ untranslated region are rapidly degraded in the cytoplasm. ARE-mediated mRNA decay (AMD) is initiated by deadenylation, and *in vitro* studies have indicated that subsequent degradation occurs in the 3′–5′ direction through a complex of exonucleases termed the exosome. An alternative pathway of mRNA degradation occurs at processing bodies, cytoplasmic foci that contain decapping enzymes, the 5′–3′ exonuclease Xrn1 and the Lsm1–7 heptamer. To determine which of the two pathways is important for AMD in live cells, we targeted components of both pathways using short interfering RNA in human HT1080 cells. We show that Xrn1 and Lsm1 are essential for AMD. On the other side, out of three exosome components tested, only knockdown of PmScl-75 caused a strong inhibition of AMD. Our results show that mammalian cells, similar to yeast, require the 5′–3′ Xrn1 pathway to degrade ARE-mRNAs.**

Keywords: AU-rich element; decapping; exosome; Lsm1; Xrn1

*EMBO reports* (2006) **7**, 72–77. doi:10.1038/sj.embor.7400572

## INTRODUCTION

The normal degradation of messenger RNAs in the cytoplasm is initiated by deadenylation, followed by exonucleolytic decay in the 3′–5′ or the 5′–3′ direction. At the 3′ end, mRNA is degraded by the exosome, a complex of six phosphorolytic 3′–5′ exonucleases and several associated hydrolytic 3′–5′ exonucleases and helicases (Mitchell & Tollervey, 2000). At the 5′ end, the 7-methyl guanosine cap is removed by the decapping complex Dcp1/Dcp2, and the mRNA body is degraded by the 5′–3′ exonuclease Xrn1 (Cougot *et al*, 2004b). Dcp1/Dcp2 and Xrn1 occur in a larger complex with the Lsm1–7 proteins, all of which colocalize at cytoplasmic foci known as processing (P)-bodies. P-bodies are believed to be the site of decapping and 5′–3′ mRNA decay (Sheth & Parker, 2003; Cougot *et al*, 2004a).

Division of Rheumatology, Immunology, and Allergy, Brigham and Women's Hospital, Harvard Medical School, Smith 608, One Jimmy Fund Way, Boston, Massachusetts 02115, USA

[+]Corresponding author. Tel: +1 617 525 1233; Fax: +1 617 525 1310;
E-mail: gstoecklin@rics.bwh.harvard.edu

**Received 6 June 2005; revised 27 September 2005; accepted 29 September 2005; published online 18 November 2005**

mRNAs containing an AU-rich element (ARE) in the 3′ untranslated region (UTR) undergo rapid ARE-mediated mRNA decay (AMD) in the cytoplasm (Chen & Shyu, 1995). *In vitro* decay studies indicate that ARE-mRNAs are degraded primarily in the 3′–5′ direction by the exosome (Chen *et al*, 2001; Mukherjee *et al*, 2002), although decapping has also been reported (Gao *et al*, 2001). ARE-binding proteins such as TTP and BRF1 were shown to interact with both the exosome and components of the decapping/5′–3′ decay pathway (Chen *et al*, 2001; Gherzi *et al*, 2004; Lykke-Andersen & Wagner, 2005). In the present study, we have quantified AMD after separately knocking down each of the two decay pathways in mammalian cells. Our results show a strong requirement for the 5′–3′ pathway, and also that the exosome component PmScl-75 participates in AMD.

## RESULTS AND DISCUSSION

### AMD is inhibited by knockdown of Xrn1

To investigate ARE-mRNA turnover in mammalian cells, we generated a stable HT1080 cell line (HTGM5) expressing a β-globin reporter gene that contains the ARE of granulocyte–macrophage colony-stimulating factor (GM-CSF) in its 3′UTR. Whereas globin mRNA lacking the ARE is stable during a 6-h period in the presence of actinomycin D, the globin-ARE mRNA is rapidly degraded (supplementary Fig S1 online). We determined the basal decay rate of globin-ARE mRNA after transiently transfecting water alone or two unspecific control short interfering RNAs (siRNAs; Fig 1A), and measured a $t_{1/2}$ of 2.3, 1.6 and 2.0 h, respectively. These values were averaged to a combined $t_{1/2}$ of 2.0 h (Table 1), which was taken as the basal decay rate.

To inhibit the 5′–3′ pathway, we targeted the principal cytoplasmic 5′–3′ exonuclease Xrn1 with two different siRNAs, thereby reducing Xrn1 protein expression to about 20% of its original level (Fig 2A). Both siRNAs inhibited AMD (Fig 1B,C), increasing the globin-ARE mRNA $t_{1/2}$ from 2.0 to 4.1 and 5.2 h, respectively (Table 1). The expression of Dcp2, the catalytically active component of the decapping complex in mammalian cells, was reduced to about 10% of its original level by two different siRNAs (Fig 2B). Knockdown of Dcp2, however, did not change the globin-ARE mRNA decay rate (Fig 1D,E). Knockdown of Dcp1a (Fig 2C), an activator of decapping in mammalian cells, had a modest but significant effect on AMD (Fig 1F), increasing the $t_{1/2}$ to 2.9 h.

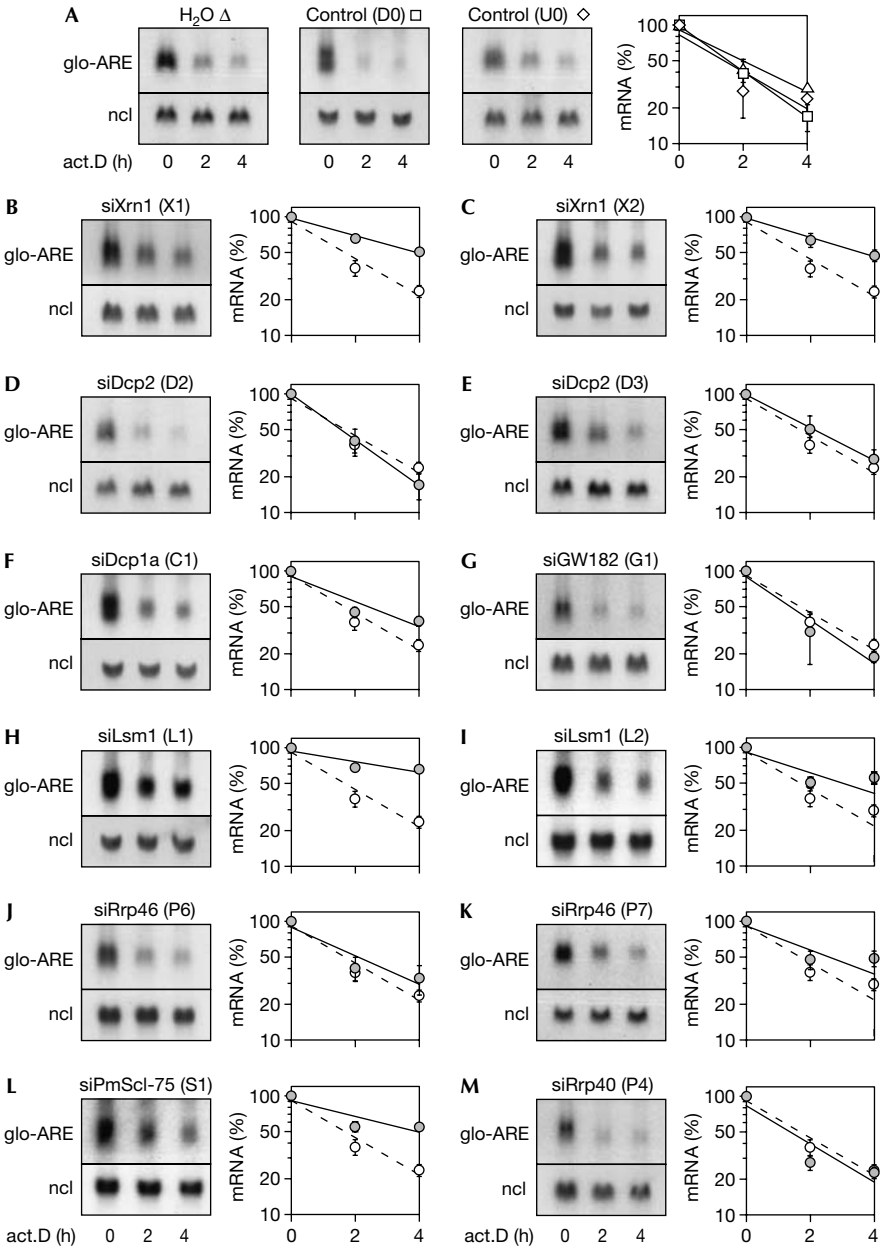


**Fig 1** | Decay of globin-ARE (AU-rich element) messenger RNA after knocking down components of the 5′–3′ and 3′–5′ decay pathways. HTGM5 cells stably express a β-globin reporter mRNA that contains the ARE of granulocyte–macrophage colony-stimulating factor in its 3′ untranslated region. Cells were transfected twice with 100 nM of short interfering RNA (siRNA) during a period of 4 days, and globin-ARE mRNA stability was assessed by actinomycin D chase experiments, followed by northern blot analysis. (**A**) The basal rate of globin-ARE mRNA decay was determined by transfection of either water alone or two unspecific control siRNAs. (**B**,**C**) Globin-ARE mRNA stability was measured after knocking down Xrn1, (**D**,**E**) Dcp2, (**F**) Dcp1a, (**G**) GW182, (**H**,**I**) Lsm1, (**J**,**K**) Rrp46, (**L**) PmScl-75 or (**M**) Rrp40. In the graphs, globin-ARE mRNA signal intensities were quantified, normalized to nucleolin mRNA and the average values ± s.e. from three to seven repeat experiments (Table 1) were plotted against time. The dashed line represents the basal globin-ARE mRNA decay rate calculated from the combined controls.

## Lsm1 is required for AMD and P-body formation

Xrn1 and the Dcp1/Dcp2 decapping enzymes are found in a complex with the Lsm1–7 proteins, which form a seven-member ring structure (Bouveret *et al*, 2000). Lsm1 is restricted to the cytoplasmic Lsm complex, whereas Lsm2–7 occur also in the nucleus as part of the spliceosome (Achsel *et al*, 1999). To specifically knock down the cytoplasmic Lsm complex, HTGM5 cells were transfected with siRNAs targeting Lsm1. As no Lsm1 antibody was available to us, efficiency of the siRNA was demonstrated on transiently transfected Flag-tagged Lsm1 immunoprecipitated with a Flag antibody (Fig 2D). Downregulation of Lsm1 by either siRNA inhibited AMD (Fig 1H,I), increasing

**Table 1** | ARE-mRNA $t_{1/2}$ after knocking down components of the 5′–3′ and 3′–5′ decay pathway

| Target | siRNA | ARE-mRNA $t_{1/2}$ (h) | s.e. | *n* | *P* (*t*-test) |
|---|---|---|---|---|---|
| Control | $H_2O$ | 2.3 | 0.11 | 5 | – |
| Control | D0 | 1.6 | 0.23 | 4 | – |
| Control | U0 | 2.0 | 0.23 | 4 | – |
| Combined | – | 2.0 | 0.14 | 13 | – |
| Xrn1 | X1 | 4.1 | 0.24 | 7 | <0.05 |
| Xrn1 | X2 | 5.2 | 1.28 | 6 | <0.05 |
| Dcp2 | D2 | 1.6 | 0.03 | 3 | 0.17 |
| Dcp2 | D3 | 2.2 | 0.35 | 4 | 0.42 |
| Dcp1a | C1 | 2.9 | 0.28 | 3 | <0.05 |
| Lsm1 | L1 | 6.9 | 0.65 | 4 | <0.05 |
| Lsm1 | L2 | 3.6 | 0.54 | 4 | <0.05 |
| GW182 | G1 | 1.7 | 0.10 | 3 | 0.28 |
| Rrp46 | P6 | 2.8 | 0.71 | 5 | 0.11 |
| Rrp46 | P7 | 3.1 | 0.53 | 3 | <0.05 |
| PmScl-75 | S1 | 4.6 | 0.34 | 4 | <0.05 |
| Rrp40 | P4 | 1.9 | 0.14 | 3 | 0.73 |

#*P*-values were determined in comparison with the combined controls.

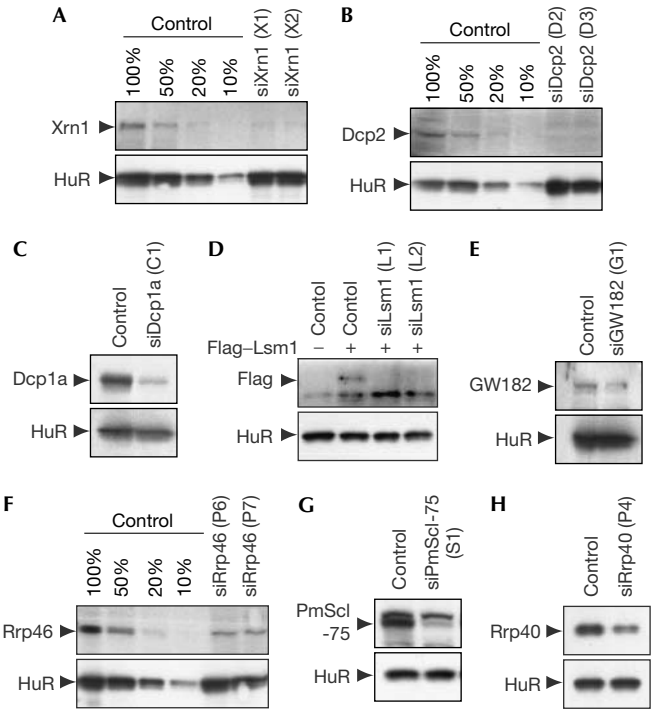


**Fig 2** | Knockdown of components of the 5′–3′ and 3′–5′ decay pathways by short interfering RNA. (**A**) HTGM5 cells were transfected twice during a period of 4 days with short interfering RNAs (siRNAs) targeting Xrn1, (**B**) Dcp2, (**C**) Dcp1a, (**D**) Lsm1, (**E**) GW182, (**F**) Rrp46, (**G**) PmScl-75 or (**H**) Rrp40. Endogenous proteins were monitored by western blot analysis except for Lsm1, in which transiently transfected Flag–Lsm1 was detected after immunoprecipitation using a Flag antibody. Where indicated, control samples were titrated to allow for quantitative estimation of knockdown efficiency.

the globin-ARE mRNA $t_{1/2}$ from 2.0 to 6.9 and 3.6 h, respectively (Table 1). Knockdown of Lsm1 also reduced the proportion of cells with visible P-bodies from 60% to 20% (Fig 3A; supplementary Fig S2 online). Knockdown of GW182 (Fig 2E), an RNA-binding protein important for P-body formation (Yang *et al*, 2004), reduced the abundance of P-bodies to a similar degree, but did not affect AMD (Fig 1G). In contrast to GW182 and Lsm1, knockdown of Dcp1a increased P-body abundance, whereas knockdown of Dcp2 had no effect (Fig 3A; supplementary Fig S2 online).

## Knockdown of PmScl-75 inhibits AMD

To determine the contribution of the 3′–5′ degradation pathway to AMD, we first targeted Rrp46, one of the phosphorolytic core exonucleases of the exosome. Two different siRNAs reduced Rrp46 expression to about 30% of its original level (Fig 2F), and caused a slight increase in the globin-ARE mRNA $t_{1/2}$ to 2.8 and 3.1 h, respectively (Fig 1J,K). Statistically, only the latter value is significantly different from the basal decay rate of 2.0 h (Table 1). As a control for exosome function, we analysed 5.8S ribosomal RNA, the nuclear processing of which requires the exosome in yeast (Mitchell *et al*, 1997). The accumulation of 5.8S rRNA precursors was observed after knockdown of Rrp46, but not in cells transfected with control siRNAs (Fig 3B). Thus, the siRNAs targeting Rrp46 effectively inhibit the exosome. PmScl-75 is another core exonuclease of the exosome, which was reported to interact directly with AREs (Mukherjee *et al*, 2002). Knockdown of PmScl-75 (Fig 2G) had the strongest effect on AMD of all exosome components tested, increasing the globin-ARE mRNA $t_{1/2}$ to 4.6 h (Fig 1L). Finally, we targeted one of the hydrolytic exonucleases of the exosome, Rrp40 (Fig 2H), which did not affect the decay rate of globin-ARE mRNA (Fig 1M). Targeting Rrp40, however, caused a stronger accumulation of 5.8S rRNA precursors than did targeting PmScl-75 (Fig 3B), indicating that the Rrp40 knockdown reduced (nuclear) exosome activity more efficiently than the PmScl-75 knockdown. Together, these data indicate that all exosome components do not participate equally in AMD, with PmScl-75 having a particularly important role.

To further explore the step at which AMD is inhibited by the different knockdowns, we analysed the polyadenylation pattern of globin-ARE mRNA (Fig 3C). In the control samples, a polyadenylated (poly(A)$^+$) mRNA population could be clearly distinguished from the poly(A)$^-$ mRNA (lanes 1–3). Knockdown of Dcp1a or Xrn1 had no visible effect on the distribution of poly(A)$^+$ and poly(A)$^-$ mRNA (lanes 4–6). In the cells transfected with siRNAs against Lsm1 and PmScl-75, however, the poly(A)$^-$ mRNA seemed to be less abundant (lanes 7–9), indicating that Lsm1 and PmScl-75 may be involved in the removal of short poly(A) tails.

## AMD primarily uses the 5′–3′ decay pathway

In this study, we show that knocking down Xrn1 strongly inhibits AMD in mammalian cells (Fig 1B,C), suggesting that 5′–3′ decay has an important role in degrading ARE-mRNAs. This result was not anticipated, as earlier *in vitro* decay studies had indicated that AMD is primarily mediated by the exosome (Chen *et al*, 2001;

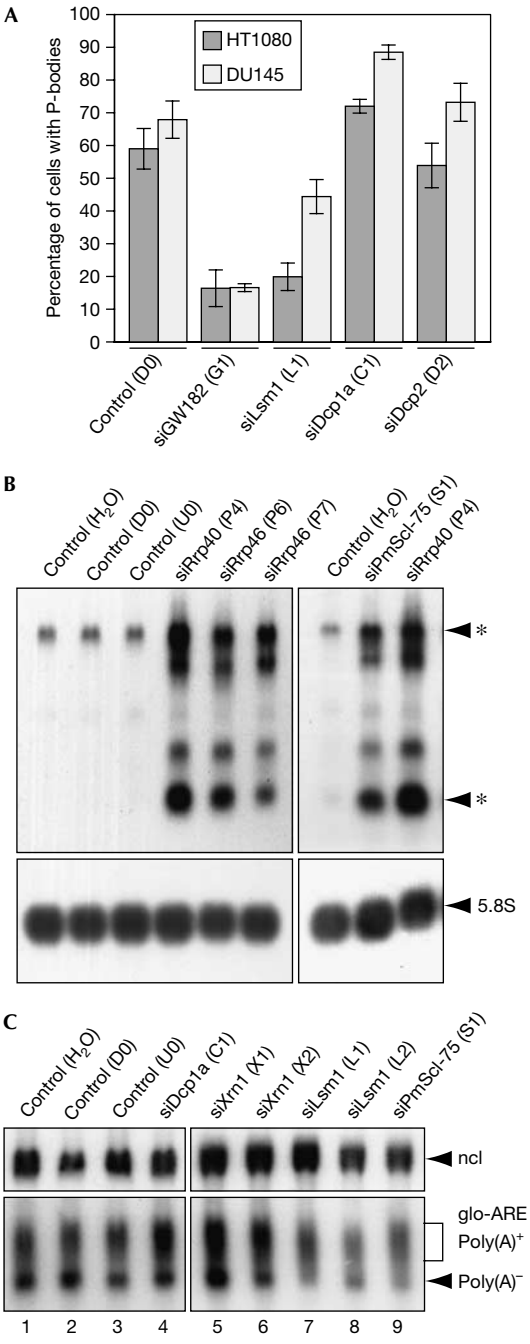


**Fig 3** | Processing-bodies, 5.8S ribosomal RNA and messenger RNA deadenylation. (**A**) Processing (P)-body abundance decreases after knocking down components of the 5′–3′ messenger RNA decay pathway. HT1080 or DU145 cells transfected once with the indicated short interfering RNAs (siRNAs) during a period of 2 days were fixed and stained for P-bodies using a commercial S6 kinase antibody that crossreacts with a component of the decapping complex (supplementary Fig S2 online). A minimum of 200 cells were scored by immunofluorescence microscopy for the presence or absence of visible P-bodies. Each transfection was repeated three or more times, and the graph shows average values ± s.e. (**B**) 5.8S ribosomal RNA precursors accumulate after knocking down exosome components. HTGM5 cells were transfected twice with the indicated siRNAs during a period of 4 days, and total RNA was analysed by northern blot using a precursor-specific probe that hybridizes 80 nt downstream of the 3′ end of 5.8S rRNA (upper panel), or an internal probe that hybridizes within 5.8S rRNA (lower panel). The principal precursor species, indicated by asterisks, probably correspond to 12S and 8S pre-rRNA. (**C**) The polyadenylation pattern of globin-ARE mRNA was analysed by northern blot after transfecting HTGM5 cells twice during a period of 4 days with siRNAs as indicated.

Mukherjee *et al*, 2002). This apparent contradiction could be attributed to the fact that decapping/5′–3′ decay complexes (that is, P-bodies) are removed or disrupted in the process of preparing cytoplasmic extracts (which usually involves an S100 ultracentrifugation step). It is important to note that the ARE was also shown to stimulate decapping *in vitro* (Gao *et al*, 2001). Moreover, our data are in good agreement with studies in *Saccharomyces cerevisiae*, in which the degradation of MFA2 and TIF51A mRNAs—which contain ARE-like motifs in their 3′UTRs—occurs through the decapping/5′–3′ decay pathway (Muhlrad *et al*, 1994; Vasudevan & Peltz, 2001). It thus seems that the directionality of AMD is conserved between yeast and mammalian cells.

Surprisingly, reducing Dcp2 levels did not inhibit AMD (Fig 1D,E). Dcp2 is the enzymatically active component of the decapping complex in mammalian cells (Lykke-Andersen, 2002; van Dijk *et al*, 2002; Wang *et al*, 2002), and knocking down Dcp2 was shown to effectively inhibit nonsense-mediated mRNA decay (Lejeune *et al*, 2003; Unterholzner & Izaurralde, 2004). As Dcp2 binds to the RNA outside the cap structure before hydrolysing the cap (Piccirillo *et al*, 2003), it is possible that Dcp2 may not recognize all mRNAs equally well. Further experiments are needed to determine whether the ARE induces decapping by a Dcp2-independent mechanism.

Among the exosome-associated 3′–5′ exonucleases tested, knockdown of Rrp46 or Rrp40 has no, or only a weak, effect on AMD (Fig 1J–M). Importantly, knockdown of Rrp46 and Rrp40 effectively inhibited the nuclear exosome, as shown by a reduction in 5.8S rRNA processing (Fig 3B). This indicates that the exosome as a complex is not of major importance for AMD in HT1080 cells. In this context, it is interesting to note that knockdown of several exosome components in *Drosophila* S2 cells does not have an effect on AMD either (Jing *et al*, 2005). Conversely, we observed that knockdown of PmScl-75 has a strong effect on AMD (Fig 1L). PmScl-75 has been shown to interact specifically with AREs (Mukherjee *et al*, 2002). Among the several isoforms reported for PmScl-75, an amino-terminally truncated form does not associate with the exosome (Raijmakers *et al*, 2003). PmScl-75 may thus have a specialized role in AMD outside of its function as an exosome component. Given that poly(A)$^-$ mRNA was less abundant in the PmScl-75 knockdown cells (Fig 3C), we speculate that PmScl-75 may be involved in the removal of short poly(A) tails.

## P-bodies may participate in AMD

Genetic studies have established that AMD requires the expression of the zinc-finger protein TTP (Carballo *et al*, 1998). In

HT1080 cells, the TTP-related protein BRF1 is essential for AMD (Stoecklin *et al*, 2002). Whereas the two highly conserved $C_3H$ zinc-finger domains of TTP and BRF1 mediate binding to the ARE (Lai *et al*, 2000), their N-terminal domains interact with both the exosome and the decapping/5′–3′ decay complex (Chen *et al*, 2001; Lykke-Andersen & Wagner, 2005). Overexpressed TTP and BRF1 colocalize with P-bodies in COS7 cells (Kedersha *et al*, 2005) and HT1080 cells (data not shown). This indicates that TTP and BRF1 may deliver their target mRNAs to P-bodies for 5′–3′ decay. Indeed, we found that knocking down Lsm1 not only inhibits AMD, but also causes P-bodies to disappear (Fig 3A). Conversely, knockdown of GW182 reduces the number of P-bodies to a similar extent without affecting AMD, suggesting that the mere presence of microscopically visible P-bodies is not a prerequisite for AMD. In this case, sub-microscopic complexes of decapping/5′–3′ decay enzymes may be sufficient for AMD.

## Coupling of deadenylation and decapping/5′–3′ decay

Whereas knockdown of Xrn1 reduces the decay rate of globin-ARE mRNA in human HT1080 cells (Fig 1B,C), it does not cause an accumulation of deadenylated mRNA (Fig 3C). Yeast mutants deleted for Xrn1, however, do show an accumulation of deadenylated mRNA (Muhlrad *et al*, 1994). Although Xrn1-dependent 5′–3′ decay appears to predominate in both systems, the coupling of deadenylation and decapping/5′–3′ decay may be different in yeast and human cells. One possibility is that AMD in human cells does not require deadenylation, that is, that decapping is induced in a deadenylation-independent fashion. The observation that TTP interacts with the decapping complex (Lykke-Andersen & Wagner, 2005) would be in agreement with such an interpretation. An alternative explanation is that deadenylation may be coupled to decapping/5′–3′ decay so tightly that inhibition of downstream steps (decapping or 5′–3′ decay) would also inhibit deadenylation. As we observed a reduced abundance of poly(A)$^-$ mRNA after knockdown of Lsm1 in HT1080 cells (Fig 3C), we speculate that the mammalian Lsm1–7 complex might have a role in such a tight coupling of deadenylation and decapping/5′–3′ decay. Such a mechanism may be related to the observation that yeast Lsm1–7 not only activates decapping but also protects the 3′ end of the mRNA from exonucleolytic trimming (He & Parker, 2000). Further studies will need to address how deadenylation and decapping/5′–3′ decay are coupled in mammalian AMD, and the precise role of Lsm1–7 in this process.

## METHODS

**Plasmids and cell lines.** Human HT1080 fibrosarcoma cells and human DU145 colon carcinoma cells were cultured in Dulbecco's modified Eagle's medium (Life Technologies, Rockville, MD, USA) supplemented with 10% fetal calf serum (Sigma, St Louis, MO, USA) and 2 mM L-glutamine, 100 U/ml penicillin and 100 μg/ml streptomycin (all from Mediatech Cellgro, Herndon, CA, USA). HT1080 cells were stably transfected with the β-globin reporter gene puroMXβ, or puroMXβ-GM-CSF-ARE containing the 51-nt-long ARE of murine GM-CSF (Stoecklin *et al*, 2000). HTGM5 is an HT1080 clone stably expressing puroMXβ-GM-CSF-ARE. Plasmid pcDNA3–Flag–Lsm1 was kindly provided by J. Lykke-Andersen (University of Colorado at Boulder, unpublished). Transfections were carried out using Lipofectamine 2000 (Life Technologies) according to the supplier's protocol.

**Short interfering RNA transfection.** HTGM5 were transfected with 100 nM siRNA duplexes using Lipofectamine 2000 (Life Technologies). After 48 h, cells were re-seeded and transfected again for another 40–44 h. siRNAs were designed using published recommendations (Reynolds *et al*, 2004) and purchased from Ambion (Austin, TX, USA). The following target sequences (sense strand) were chosen:

U0: 5′-GAAUGCUCAUGUUGAAUCA-3′;
D0: 5′-GCAUUCACUUGGAUAGUAA-3′;
D2: 5′-GAAAUUGCCUUGUCAUAGA-3′;
D3: 5′-GUAUCAAGAUUCACCUAAU-3′;
L1: 5′-CAAACUUAGUGCUACAUCA-3′;
L2: 5′-CCAGCAAGUAUCCAUUGAA-3′;
X1: 5′-UGAUGAUGUUCACUUUAGA-3′;
X2: 5′-AGAUGAACUUACCGUAGAA-3′;
C1: 5′-GCAAGCUUGUCGAUAUAUA-3′;
G1: 5′-CCGGTTCAGUGCAGAAUAA-3′;
P4: 5′-GAAUAUGGGUUAAGGCAAA-3′;
P6: 5′-GCAAAGAGAUUUUCAACAA-3′;
P7: 5′-CAACACGUCUUCCGUUUCU-3′;
S1: 5′-GCGUGAUCCUGUACCAUUA-3′.

**Western blot analysis.** Total cell lysates were prepared using sample buffer, and resolved on 4–20% polyacrylamide gradient Tris–glycine gels (Invitrogen, Carlsbad, CA, USA), as described previously (Kedersha *et al*, 2000). Flag–Lsm1 was immunoprecipitated with mouse anti-Flag antibody (M2; Sigma), and the following antibodies were used for western blotting: rabbit anti-Flag (Sigma), rabbit anti-Dcp1a and rabbit anti-Xrn1 (Lykke-Andersen & Wagner, 2005), affinity-purified rabbit anti-Dcp2 (Wang *et al*, 2002), human anti-GW182 (Yang *et al*, 2004), rabbit anti-Rrp40 and rabbit anti-Rrp46 (Brouwer *et al*, 2001) and rabbit anti-PmScl-75 (Chen *et al*, 2001; Mukherjee *et al*, 2002).

**Northern blot analysis.** siRNA-transfected HTGM5 cells were treated with 5 μg/ml actinomycin D (Sigma) for 0, 2 and 4 h, and cytoplasmic RNA was extracted as described previously (Stoecklin *et al*, 2000). RNA (10–20 μg) was resolved by 1.1% agarose/formaldehyde gel electrophoresis, and β-globin was detected as described previously (Stoecklin *et al*, 2004). The nucleolin probe was generated by PCR using primers G83/G84. To analyse 5.8S rRNA, 2–8 μg of total RNA was extracted using Trizol LS (Invitrogen) and resolved on 1.5% agarose/formaldehyde gels. Membranes were hybridized at 42 °C with digoxigenin-labelled oligonucleotides G178 (5.8S rRNA) and G181 (5.8S pre-rRNA).

**DNA oligonucleotides.** DNA oligonucleotides were as follows:

G83: 5′-TTACAAAGTCACTCAGGATG-3′;
G84: 5′-AGCTTCTTTAGCGTCTTCG-3′;
G178: 5′-AGCTAGCTGCGTTCTTCATCGAC-3′;
G181: 5′-TGCGCTTAGGGGGACGGAGG-3′.

**Immunofluorescence microscopy.** HT1080 or DU145 cells were seeded onto glass coverslips, transfected with siRNA duplexes and processed for immunofluorescence 48 h later, as described previously (Kedersha *et al*, 2000). P-bodies were stained using a rabbit anti-Dcp1a antibody (Lykke-Andersen & Wagner, 2005) and a mouse anti-S6 kinase antibody (sc-8416; Santa Cruz Biotechnology, Santa Cruz, CA, USA) that crossreacts with a component of the decapping complex (supplementary Fig S2 online). Images were taken on a Nikon Eclipse E800 microscope using a CCD-Spot RT digital camera.

**Supplementary information** is available at *EMBO reports* online (http://www.emboreports.org).

ACKNOWLEDGEMENTS

We thank J. Lykke-Andersen (University of Colorado at Boulder), Ger J.M. Pruijn and R. Raijmakers (University of Nijmegen, Netherlands), M. Kiledjian and X. Jiao (Rutgers University, New Jersey), J. Wilusz (Colorado State University, Fort Collins) and M.J. Fritzler (University of Calgary, Canada) for generously providing reagents. We are also grateful to N. Kedersha (Brigham and Women's Hospital, Boston, MA) for helpful comments on the manuscript, and R. Parker (University of Arizona, Tuscon) for inspiring discussions. P.A. was supported by National Institute of Health grants AI-33600 and AI-50167. G.S. was the recipient of a stipend from the Swiss National Science Foundation.

REFERENCES

Achsel T, Brahms H, Kastner B, Bachi A, Wilm M, Luhrmann R (1999) A doughnut-shaped heteromer of human Sm-like proteins binds to the 3′-end of U6 snRNA, thereby facilitating U4/U6 duplex formation *in vitro*. *EMBO J* **18:** 5789–5802

Bouveret E, Rigaut G, Shevchenko A, Wilm M, Seraphin B (2000) A Sm-like protein complex that participates in mRNA degradation. *EMBO J* **19:** 1661–1671

Brouwer R, Allmang C, Raijmakers R, van Aarssen Y, Egberts WV, Petfalski E, van Venrooij WJ, Tollervey D, Pruijn GJ (2001) Three novel components of the human exosome. *J Biol Chem* **276:** 6177–6184

Carballo E, Lai WS, Blackshear PJ (1998) Feedback inhibition of macrophage tumor necrosis factor-α production by tristetraprolin. *Science* **281:** 1001–1005

Chen CY, Gherzi R, Ong SE, Chan EL, Raijmakers R, Pruijn GJ, Stoecklin G, Moroni C, Mann M, Karin M (2001) AU binding proteins recruit the exosome to degrade ARE-containing mRNAs. *Cell* **107:** 451–464

Chen C-YA, Shyu A-B (1995) AU-rich elements: characterization and importance in mRNA degradation. *Trends Biochem Sci* **20:** 465–470

Cougot N, Babajko S, Seraphin B (2004a) Cytoplasmic foci are sites of mRNA decay in human cells. *J Cell Biol* **165:** 31–40

Cougot N, van Dijk E, Babajko S, Seraphin B (2004b) Cap-tabolism. *Trends Biochem Sci* **29:** 436–444

Gao M, Wilusz CJ, Peltz SW, Wilusz J (2001) A novel mRNA-decapping activity in HeLa cytoplasmic extracts is regulated by AU-rich elements. *EMBO J* **20:** 1134–1143

Gherzi R, Lee KY, Briata P, Wegmuller D, Moroni C, Karin M, Chen CY (2004) A KH domain RNA binding protein, KSRP, promotes ARE-directed mRNA turnover by recruiting the degradation machinery. *Mol Cell* **14:** 571–583

He W, Parker R (2000) Functions of Lsm proteins in mRNA degradation and splicing. *Curr Opin Cell Biol* **12:** 346–350

Jing Q, Huang S, Guth S, Zarubin T, Motoyama A, Chen J, Di Padova F, Lin SC, Gram H, Han J (2005) Involvement of microRNA in AU-rich element-mediated mRNA instability. *Cell* **120:** 623–634

Kedersha N, Cho MR, Li W, Yacono PW, Chen S, Gilks N, Golan DE, Anderson P (2000) Dynamic shuttling of TIA-1 accompanies the recruitment of mRNA to mammalian stress granules. *J Cell Biol* **151:** 1257–1268

Kedersha N, Stoecklin G, Ayodele M, Yacono P, Lykke-Andersen J, Fitzler MJ, Scheuner D, Kaufman RJ, Golan DE, Anderson P (2005) Stress granules and processing bodies are dynamically linked sites of mRNP remodeling. *J Cell Biol* **169:** 871–884

Lai WS, Carballo E, Thorn JM, Kennington EA, Blackshear PJ (2000) Interactions of CCCH zinc finger proteins with mRNA. Binding of tristetraprolin-related zinc finger proteins to Au-rich elements and destabilization of mRNA. *J Biol Chem* **275:** 17827–17837

Lejeune F, Li X, Maquat LE (2003) Nonsense-mediated mRNA decay in mammalian cells involves decapping, deadenylating, and exonucleolytic activities. *Mol Cell* **12:** 675–687

Lykke-Andersen J (2002) Identification of a human decapping complex associated with hUpf proteins in nonsense-mediated decay. *Mol Cell Biol* **22:** 8114–8121

Lykke-Andersen J, Wagner E (2005) Recruitment and activation of mRNA decay enzymes by two ARE-mediated decay activation domains in the proteins TTP and BRF-1. *Genes Dev* **19:** 351–361

Mitchell P, Tollervey D (2000) Musing on the structural organization of the exosome complex. *Nat Struct Biol* **7:** 843–846

Mitchell P, Petfalski E, Shevchenko A, Mann M, Tollervey D (1997) The exosome: a conserved eukaryotic RNA processing complex containing multiple 3′→5′ exoribonucleases. *Cell* **91:** 457–466

Muhlrad D, Decker CJ, Parker R (1994) Deadenylation of the unstable mRNA encoded by the yeast MFA2 gene leads to decapping followed by 5′→3′ digestion of the transcript. *Genes Dev* **8:** 855–866

Mukherjee D, Gao M, O'Connor JP, Raijmakers R, Pruijn G, Lutz CS, Wilusz J (2002) The mammalian exosome mediates the efficient degradation of mRNAs that contain AU-rich elements. *EMBO J* **21:** 165–174

Piccirillo C, Khanna R, Kiledjian M (2003) Functional characterization of the mammalian mRNA decapping enzyme hDcp2. *RNA* **9:** 1138–1147

Raijmakers R, Egberts WV, van Venrooij WJ, Pruijn GJ (2003) The association of the human PM/Scl-75 autoantigen with the exosome is dependent on a newly identified N terminus. *J Biol Chem* **278:** 30698–30704

Reynolds A, Leake D, Boese Q, Scaringe S, Marshall WS, Khvorova A (2004) Rational siRNA design for RNA interference. *Nat Biotechnol* **22:** 326–330

Sheth U, Parker R (2003) Decapping and decay of messenger RNA occur in cytoplasmic processing bodies. *Science* **300:** 805–808

Stoecklin G, Ming XF, Looser R, Moroni C (2000) Somatic mRNA turnover mutants implicate tristetraprolin in the interleukin-3 mRNA degradation pathway. *Mol Cell Biol* **20:** 3753–3763

Stoecklin G, Colombi M, Raineri I, Leuenberger S, Mallaun M, Schmidlin M, Gross B, Lu M, Kitamura T, Moroni C (2002) Functional cloning of BRF1, a regulator of ARE-dependent mRNA turnover. *EMBO J* **21:** 4709–4718

Stoecklin G, Stubbs T, Kedersha N, Wax S, Rigby WF, Blackwell TK, Anderson P (2004) MK2-induced tristetraprolin:14-3-3 complexes prevent stress granule association and ARE-mRNA decay. *EMBO J* **23:** 1313–1324

Unterholzner L, Izaurralde E (2004) SMG7 acts as a molecular link between mRNA surveillance and mRNA decay. *Mol Cell* **16:** 587–596

van Dijk E, Cougot N, Meyer S, Babajko S, Wahle E, Seraphin B (2002) Human Dcp2: a catalytically active mRNA decapping enzyme located in specific cytoplasmic structures. *EMBO J* **21:** 6915–6924

Vasudevan S, Peltz SW (2001) Regulated ARE-mediated mRNA decay in *Saccharomyces cerevisiae*. *Mol Cell* **7:** 1191–1200

Wang Z, Jiao X, Carr-Schmid A, Kiledjian M (2002) The hDcp2 protein is a mammalian mRNA decapping enzyme. *Proc Natl Acad Sci USA* **99:** 12663–12668

Yang Z, Jakymiw A, Wood MR, Eystathioy T, Rubin RL, Fritzler MJ, Chan EK (2004) GW182 is critical for the stability of GW bodies expressed during the cell cycle and cell proliferation. *J Cell Sci* **117:** 5567–5578